Materials Science and Engineering C 29 (2009) 1609–1615

Contents lists available at ScienceDirect

Materials Science and Engineering C

journal homepage: www.elsevier.com/locate/msec

Binding affinity of fluorochromes and fluorescent proteins to Taxol™ crystals

Javier S. Castro [a,*], Bartosz Trzaskowski [b,1], Pierre A. Deymier [a], Jaim Bucay [a], Ludwik Adamowicz [b], James B. Hoying [c]

[a] Department of Materials Science and Engineering, University of Arizona, Tucson AZ 85721, United States
[b] Department of Chemistry, University of Arizona, Tucson AZ 85721, United States
[c] Cardiovascular Innovation Institute, University of Louisville, Louisville KY 40202, United States

ARTICLE INFO

Article history:
Received 30 November 2008
Accepted 17 December 2008
Available online 31 December 2008

Keywords:
Taxol crystals
Spherulites
Tubulin
Fluorochromes
Binding energy
Computational docking

ABSTRACT

The ability of Taxol (paclitaxel) to bind and stabilize microtubules is the basis for its use as an anti-mitotic drug as well as an additive for *in vivo* and *in vitro* studies of microtubules. The low solubility of Taxol in aqueous solutions, however, facilitates the formation of Taxol crystals that can be decorated with fluorescent tubulin. In cells treated with Taxol, these decorated Taxol crystals may be mistaken for self-assembled tubulin asters when observed with a fluorescent microscope. We confirmed via fluorescent and differential interference contrast microscopy that Taxol crystals can be decorated not only with fluorescent tubulin but also with other fluorescent proteins and fluorochromes without perturbing their morphology. We used theoretical calculations to further investigate Taxol-fluorescent agent interactions. Using computational docking studies we identified a new, potential Taxol binding site within the tubulin dimmer, allowing the interaction between crystalline Taxol and tubulin. Our calculations, however, show that fluorescent tubulin binding to Taxol crystals is more favorable via the fluorochromes covalently linked to the tubulin dimmers, rather than via the new Taxol-binding site, what is in accordance with our experimental data.

1. Introduction

Taxol (paclitaxel, Fig. 1), a small molecule originally isolated from the needles and bark of the Pacific Yew tree (*Taxus brevifolia*), has been one of the most successful anti-cancer drugs [1]. Taxol's role in arresting the growth of tumors is a result of its ability to bind to and stabilize microtubules (MTs) in the cytoplasm, preventing mitosis [2–4]. Stabilization is a result of Taxol binding preferentially to the inner surface of the microtubule [5,6]. In studies of cells treated with Taxol, several groups have reported the presence of complex microtubule morphologies, not found in normal cells, such as bundles and asters (structures that emulate the mitotic spindle). These structures are transparent and can only be observed using fluorescent microscopy after immunofluorescent labeling of MTs. There has been a consensus theory that Taxol is the main inducer of these structures [7–11]. On the other hand, studies using supersaturated aqueous solutions of the drug, have shown that Taxol crystallizes in the form of needles [12,13] forming complex morphologies such as spherulitic crystals [14]. These Taxol crystals have some morphological similarities to the structure of MTs, e.g. sizes and shapes.

Recently, the nature of MT asters found in cells treated with Taxol have been questioned by Foss et al.[15], who have reported that fluorescent tubulin can bind to Taxol needles and spherulites in vitro. Foss et al. suggested that microtubule asters and bundles observed in cells treated with Taxol could in fact be Taxol spherulites or needles decorated with fluorescent tubulin, mimicking microtubule structures when observed with the fluorescence microscope. This hypothesis has not been definitively validated yet, therefore it is critical to clarify the interaction between Taxol crystals and florescent tubulin in order to ascertain the nature of these filamentous structures observed in cells treated with Taxol. This problem is particularly important for in-vivo studies, since Taxol concentrations used in cellular studies may exceed its solubility limit of 0.77 μM [16].

On the other hand the interaction between tubulin and Taxol has been widely studied in vitro and *in vivo*, and detailed descriptions of the binding affinity of Taxol to tubulin dimers can be found in the literature. To date it is known that Taxol only binds to polymerized tubulin (microtubules) at a very specific site. To our knowledge, however, the inverse process in which unpolymerized tubulin dimers may bind to crystallized Taxol has not been explored yet. Although Foss et al show experimental evidence of the interaction of fluorescent tubulin with Taxol crystals, they do not provide further analysis of this phenomenon.

In this paper we explored two different hypotheses for the binding of fluorescent tubulin to Taxol crystals. The first one is a new potential Taxol-binding site within the tubulin dimer. The second hypothesis

* Corresponding author. 1235 E. James E. Rogers way, Tucson, AZ 85721, United States. Tel.: +1 520 621 6070; fax: +1 520 621 8059.
E-mail address: jscastro@email.arizona.edu (J.S. Castro).
[1] Current address: Materials and Process Simulation Center, California Institute of Technology, Pasadena CA 91125.

0928-4931/$ – see front matter © 2008 Elsevier B.V. All rights reserved.
doi:10.1016/j.msec.2008.12.026

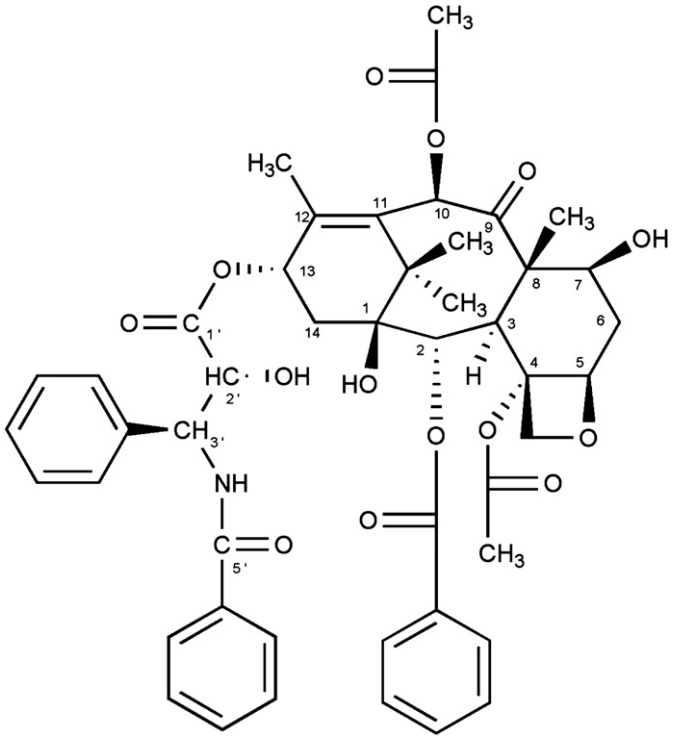

Fig. 1. Taxol molecule with numbering scheme.

assumes that tubulin dimers are interacting with Taxol via the covalently attached fluorochrome. We conducted several experiments in aqueous solutions where Taxol crystals were grown and exposed to different solutions containing flourescent proteins; rhodamine tubulin and rhodamine actin or only flourochromes; rhodamine, Cy3 (from the cyanine dye family) and Alexa Fluor 488, to better understand the binding interaction between flourescent proteins and Taxol crystals. The morphology of the observed structures was analyzed via fluorescent microscopy, differential interference contrast (DIC) microscopy and field emission scanning electron microscopy (FESEM). Experimental studies were complemented by computational docking and semi-empirical investigations of Taxol crystal structure and its affinity for tubulin and fluorochromes.

2. Results and discussion

2.1. Experimental results

To investigate the binding of fluorescent proteins and fluorochromes to Taxol spherulites, we crystallize taxol in a microtubule assembly buffer using a concentration of 100 μM. This Taxol concentration produced spherulitic crystals that were relatively easy to observe. Because these crystals are transparent we used DIC microscopy for their morphological characterization, observing Taxol aggregates exhibiting sheaf-like and spherulitic morphologies as shown in Fig. 2a. This pre-formed Taxol spherulites containing buffer (Tx-Buffer) was then used to investigate the interaction of Taxol crystals with fluorescent molecules.

First, we combined the Tx-Buffer with fluorescent tubulin as described in the methods section. In order to accurately determine if the fluorescent tubulin had bound to the spherulites, it was necessary to conduct a thorough rinse to remove any unbound molecules and fluorescent background. The sample was then analyzed with a fluorescent microscope with which we observed fluorescent spherulites with analogous morphologies to those grown in pure Tx-Buffer (Fig. 2b). These results indicate, as Foss et al. reported, that fluorescent tubulin can bind to Taxol crystals. As we have mentioned before, however, there is no further explanation of how fluorescent tubulin interacts with these crystals. Therefore, two possibilities should be explored; the binding of fluorescent proteins to crystallized Taxol through the direct attachment of the protein to Taxol or via the fluorochrome covalently attached to the protein.

To shed light on the binding interaction between rhodamine tubulin and Taxol crystals we conducted an experiment using rhodamine actin in place of the rhodamine–tubulin conjugate. It is similar fluorescent cytoskeletal protein, but no binding between this system and Taxol has been reported up to date [17,18]. We observed fluorescent spherulites with no visible morphological differences to those labeled with rhodamine tubulin (Fig. 2c).

Although the binding of the rhodamine actin conjugate to Taxol spherulites does not completely discard a direct tubulin–spherulite interaction, it suggests the direct binding of rhodamine to Taxol when conjugated rhodamine is used. To support this, we combined the Tx-Buffer with pure rhodamine, as described in the methods section. We observed fluorescent spherulites morphologically identical to those previously found in the fluorescent protein solutions (Fig. 2d), confirming that rhodamine does indeed bind to Taxol spherulites.

Finally, we explored the possibility of other fluorochromes binding to Taxol spherulites. For this, we used two different fluorochromes, Cy3 and a conjugated Alexa Fluor 488 goat anti-mouse, following the same protocol of the preceding experiments. We observed identical fluorescent spherulites to those labeled with rhodamine (Figs. 2e–f), indicating that Taxol spherulites can be decorated not only with fluorescent tubulin, as Foss et al. reported, but also with other fluorescent proteins, fluorochromes and fluorochrome-conjugates.

2.2. FESEM characterization

We further characterized Taxol spherulites by means of Field Emission Scanning Electron Microscopy (FESEM). Three samples were analyzed; one containing unlabeled spherulites, and the other two containing labeled spherulites with rhodamine tubulin and pure rhodamine. No visible differences were found among all these samples. Each showed needle-like crystals with a broad range of diameters ranging from 45 to 720 nm, and lengths exceeding 10 μm (Fig. 3a). At high magnifications the crystals' topography was smooth with no apparent differences between the various samples (Fig. 3b and c).

2.3. Computational analysis

In addition to the experimental results we performed a theoretical analysis of Taxol's crystal structure and its binding affinity with tubulin and fluorescent molecules. In order to analyze the possible binding affinity of Taxol crystals with other molecules, it is necessary to understand the crystal structure of Taxol. The analysis of the three-dimensional arrangement of Taxol molecules reveals that the molecules of Taxol form two different kinds of hydrogen-bonded dimers [19] (Figs. 1, 4a–b). The specific interactions stabilizing the system in the first dimer are between the O7 atom of the first molecule of the dimer (A) and O2′atom of the second molecule of the dimer (B) as well as O2′(A) and C10(B) atoms (Fig. 4b). The second type of dimer is stabilized by the hydrogens bond between O1(A) and C2(B) atoms and C2(A) and O1(B) atoms. Additionally dimers are linked together by hydrogen bonds between the O5′(A) carbonyl oxygen and O7(B) hydroxyl group to form a three-dimensional structure. The first two pairs of hydrogen bonds and the 2-fold screw axis of the crystal result in a ribbon-like structure of Taxol dimers with the diameter below 1 nm. The additional single hydrogen bond between dimers forming the ribbon-like structure allows packing the ribbons into a three-dimensional structure. We can hypothesize that the single hydrogen bond between the C5′(A) carbonyl oxygen and the O7(B) hydroxyl group is probably too weak to stabilize the three-

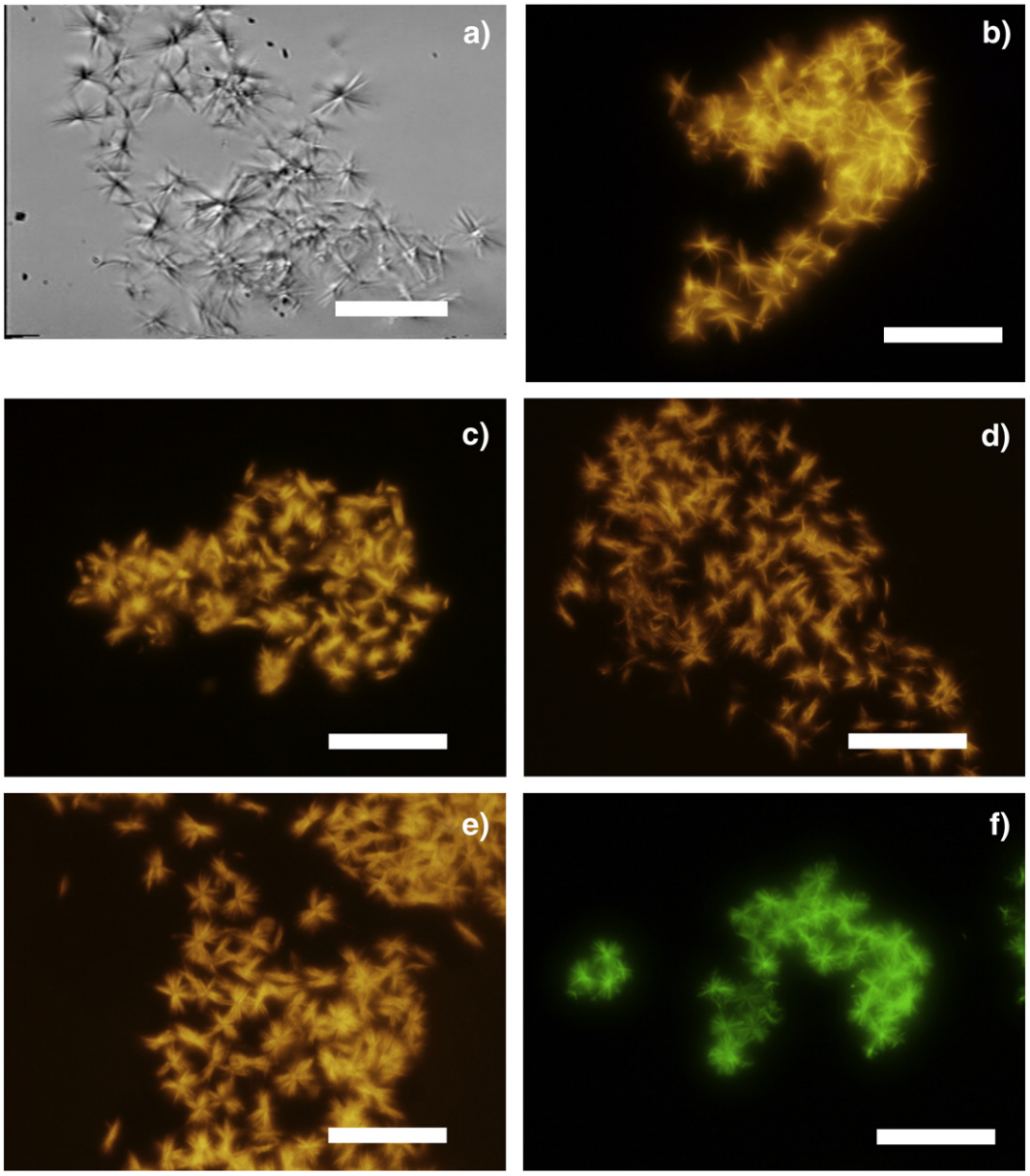

Fig. 2. Taxol spherulites grown in a microtubule assembly buffer. a) Unlabeled Taxol spherulites, observed with DIC microscopy. Fluorescent images of Taxol spherulites labeled with: b) rhodamine tubulin, c) rhodamine actin, d) rhodamine, e) Cy3 and f) Alexa Fluor 488. Bars 20 μm.

dimensional structure of Taxol crystals over large distances. In such case the result would be a set of small numbers of Taxol ribbons interacting laterally to form needle-like structures of different diameter. The diameter of these structures would depend on the number of bundled Taxol ribbons. This hypothesis may explain the broad range of filament's diameters found in the FESEM images.

The possible binding of tubulin dimers to Taxol crystals, found in the experimental section of this work, is not likely via the known Taxol-binding site. Taxol bound to the known Taxol-binding site of the tubulin dimer is almost completely buried inside this site and there are no available chemical groups able to form hydrogen bonds to form a crystal lattice, which are exposed to the solution (Fig. 5a) [20]. The O2′ hydroxyl oxygen atom is buried deep in the binding pocket and interacting with pro 360 and gly 370 of the B9-B10 loop of the tubulin dimer, while O7 hydroxyl oxygen and C10 acetyl oxygen are very close to the B7-H9 M-loop. The three remaining Taxol atoms stabilizing the crystal lattice by the formation of hydrogen bonds (O1 hydroxyl oxygen, C2 benzoyl oxygen and C5′ carbonyl oxygen) are close to his 229 residue of the H7 alpha-helix. This simple geometrical analysis allowed us to exclude the known native Taxol-binding binding site as being responsible for Taxol crystal-tubulin interaction and put forward two hypotheses. The first one implies that there is another Taxol-binding site within the tubulin dimer, while in the second hypothesis tubulin dimers are interacting with Taxol via a fluorescent agent, which is covalently attached to them.

To verify the first hypothesis we used a theoretical approach described in the computational methods section. The first step, rigid docking, allowed us to define four new sites in the tubulin dimer, which had very high scores of the geometrical matching between them and the Taxol molecule. Two of those sites had high similarity towards the tubulin-Taxol conformation, while two other sites had high similarity towards Taxol in its native conformation found in water solution. We evaluated the hydrophobicity of those four sites, and all of them were found to be highly hydrophobic, which suggested strong interaction between them and the lipophilic Taxol molecule.

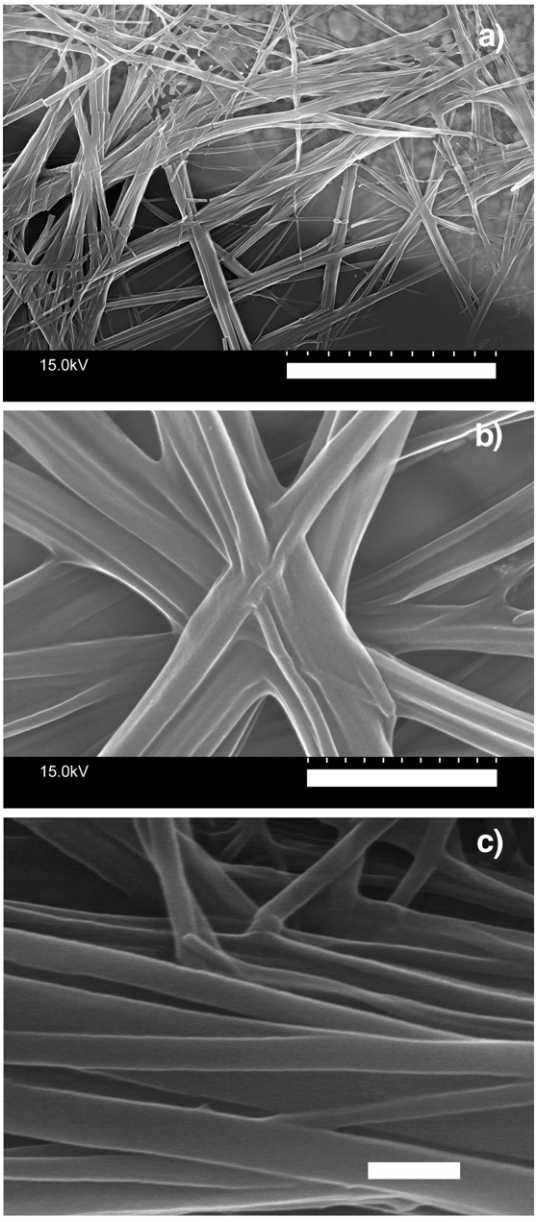

Fig. 3. Taxol spherulites analyzed by FESEM. Pure Taxol crystals a) low magnification, bar 10 μm b) high magnification, bar 1 μm c) Taxol crystals with rhodamine tubulin, high magnification, bar 500 nm. Extraction voltage 15 kV.

In the last step of this computational part we used the Autodock software binding energy evaluations and compared the results to the native Taxol-binding site. Three out of four candidates for new binding sites had large positive binding energies due to unfavorable interactions between the hydrophobic Taxol and charged or hydrophilic amino acid residues. For the last site, however, Autodock calculations suggested that the binding energy is favorable and is approximately two times lower than the binding energy of the original native Taxol-binding site (-16.75 kJ/mol versus -33.66 kJ/mol for the original native Taxol site). This result allows us to suggest that this site has a relatively high affinity towards the Taxol molecule and, in the presence of high Taxol concentration, may bind Taxol molecules.

The new candidate for the Taxol-binding site is situated in a small groove located on the boundary between alpha-tubulin and beta-tubulin in the tubulin dimer. The binding geometry may be characterized by five hydrogen bonds between the Taxol molecule and the tubulin dimer (Fig. 5b). Three of those possible hydrogen bonds are interactions between amino acid residues of the alpha monomer; these are the interactions between the amide nitrogen atom of gln 176 and O13 oxygen atom, the guanidinium nitrogen atom of arg 214 and O5 oxygen atom and the amine nitrogen atom of lysine 304 and O5′ carbonyl oxygen atom. Beta-tubulin adds another two possible hydrogen bonds: between the amide nitrogen atom of asn 334 and O7 hydroxyl oxygen atom and the amide nitrogen atom of ASN 337 and O4 oxygen atom. Some of the oxygen atoms needed to form hydrogen bonds to form a crystal lattice (O7 hydroxyl oxygen, C10 acetyl oxygen and C5′ carbonyl oxygen) are occupied or buried deep within the binding site. On the other hand the remaining oxygen atoms responsible for the stabilization of the Taxol crystal structure (O2′ hydroxyl oxygen, O1 hydroxyl oxygen and C2 benzoyl oxygen) are relatively far from the protein. These atoms are free to form the hydrogen bond net with other Taxol molecules, which are forming the crystal lattice. The conformation of the Taxol molecules in the new binding site resembles its native conformation in the solution of water and dimethyl sulfoxide (DMSO), with the distances of 5.4 Å and 9.8 Å between the benzene aromatic rings [21]. It is important to notice, however, that the tubulin binding via the new Taxol-binding site would not be possible if the Taxol crystal had existed in form of perfect, defect-free Taxol ribbons. In such case neither O7 hydroxyl oxygen nor C10 acetyl oxygen atoms would be exposed to the solution and able to bind tubulin dimers, but would be interacting with other Taxol molecules of the crystal lattice. We believe, however, that there is a possibility of defects in the needle-like structure of Taxol crystals, particularly at the outermost Taxol ribbons. The defects are probably due to the different strengths of the hydrogen bonds stabilizing crystalline Taxol and may look like steps at the peripheries of Taxol crystals. These steps should be two Taxol dimers high in order to expose to the solution the chemical groups that are able to bind tubulin dimer or other biomacromolecule.

The second hypothesis investigated in this work is the tubulin-Taxol binding via the fluorescent agent attached covalently to the tubulin dimer. To test this premise we have used the semi-empirical calculations of rhodamine-Taxol system (used in this work) and fluoroescein-Taxol system (used in the work of Foss el. al. [16]), as described in the computational methods section. For both fluorescent agents we found that the most favorable geometry involves a hydrogen bond between the C5′ carbonyl oxygen of Taxol and O1 xanthene oxygen of rhodamine/fluorescein (Fig. 4c). The PM6 evaluation of the interaction energies between fluorescein and Taxol gives a value of −94.20 kJ/mol (−53.17 kJ/mol in the case of a protonated fluorescein), while for the rhodamine-Taxol system it's −45.22 kJ/mol (−30.56 kJ/mol for the protonated rhodamine). These values indicate that the interaction between Taxol and the two fluorescent agents is favorable from the energetic point of view.

The results of our calculations suggest that the second hypothesis is the more likely explanation of the experimental data presented in this work. First, the interaction energy between Taxol and fluorescein/rhodamine systems is evaluated to be more favorable than the interaction energy between Taxol and the new binding site within the tubulin dimer. Second, the interaction between Taxol and fluorescein/rhodamine, which involves the C5′ carbonyl oxygen of Taxol, is possible for both a defect-free and defective crystal. Given all the data presented in this work we cannot, however, completely discard the possibility of a new, second Taxol-binding site in the tubulin system.

2.4. Conclusions

The structural analysis of the Taxol crystal suggests that Taxol molecules, although bound in the crystal lattice, still have some of their functional groups exposed to the solution resulting in their biological activity. Therefore it would be expected that Taxol crystals may interact with other molecules as well. Using computational docking studies we identified a new, potential Taxol binding site within the tubulin dimmer, in which Taxol molecule is only partially embedded in the protein allowing the interaction between crystalline Taxol and tubulin. Our calculations, however, show that fluorescent

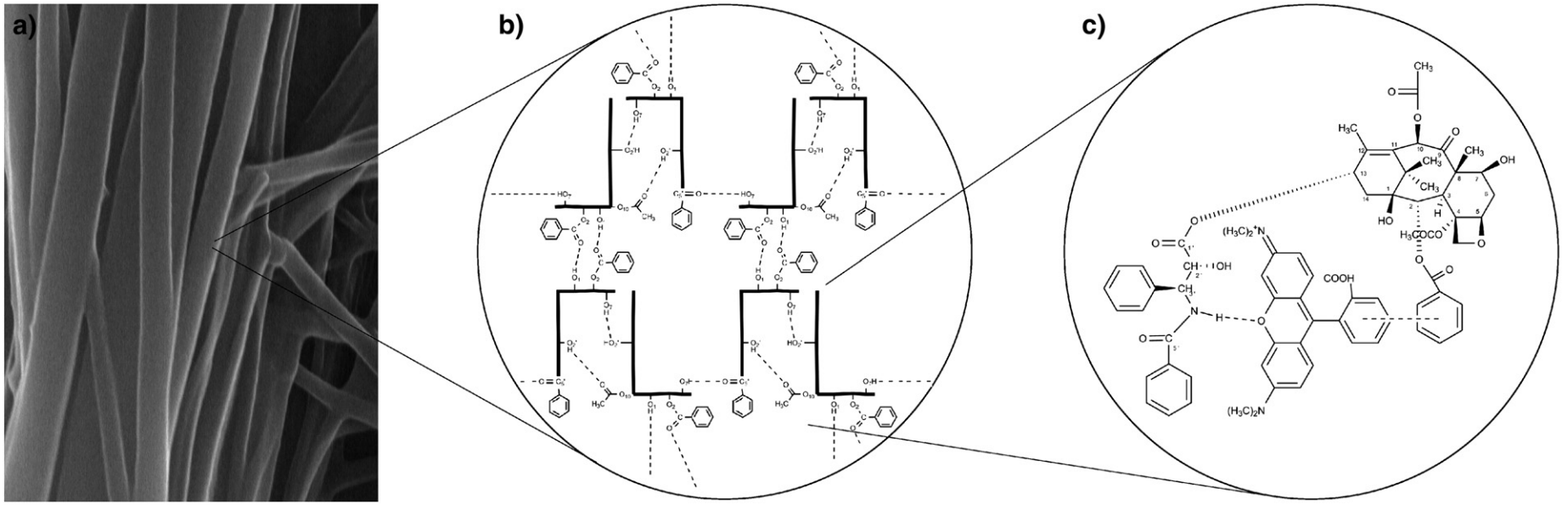

Fig. 4. Schematic diagram of hydrogen bonds between Taxol molecules in crystal lattice and in a Taxol-rhodamine model. a) Taxol spherulites with rhodamine-tubulin analyzed by FESEM. b) Schematic representation of hydrogen bond network in Taxol crystals. Each Taxol molecule is depicted with a horizontal line representing the rigid ring structure and a vertical line representing the C13 side chain tail. Dashed lines represent hydrogen bonds, while gray lines show borders between Taxol ribbons connected to each other via the O5′–O7 hydrogen bond. (c) Schematic representation of the optimized structure of Taxol-tetramethylrhodamine model with dashed lines representing the most important interactions.

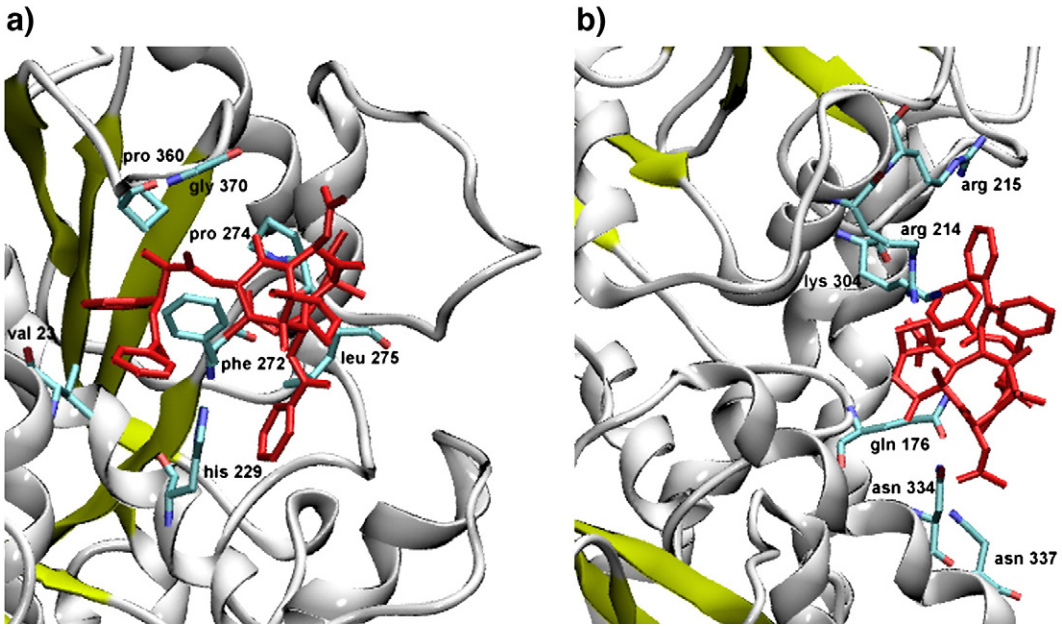

Fig. 5. Details of Taxol-binding sites. (a) The native Taxol-binding site in the beta-tubulin monomer. (b) The new candidate for Taxol-binding site in the groove between alpha-tubulin and beta-tubulin monomers. This figure was created using VMD [30].

tubulin binding to Taxol crystals is more favorable via the fluorochromes covalently linked to the tubulin dimmers, rather than via the new Taxol-binding site. These results are substantiated by our experimental findings that strongly suggest the binding of fluorescent proteins to Taxol crystals as a result of the direct interaction of fluorochromes with Taxol and not the direct attachement of proteins [15]. This high-affinity binding between taxol spherulites and fluorochromes is very important when immunolabeling is utilized for targeting microtubules in cells treated with taxol, since fluorescent molecules could bind to crystallized Taxol, thus mimicking microtubules asters or bundles when analyzed by fluorescent microscopy.

3. Materials and methods

3.1. Materials

The following materials were used: PEM80 buffer (80 mM PIPES, 0.5 mM EGTA, 4 mM $MgCl_2$), paclitaxel (Taxol) diluted in DMSO at 2 mM, fluorescent rhodamine tubulin from bovine brain (cat. #T331M), tubulin protein from bovine brain (Cat. # TL238), non-muscle rhodamine actin from human platelets (Cat. # APHR) and guanosine 5′ triphosphate (GTP) all these materials were purchased from Cytoskeleton®. From Invitrogen® we used Tetramethyl-rhodamine (TMR) (cat. # C1171) and a conjugate Alexa fluor 488 goat anti-mouse (cat. # A-411001). Finally we used Cy3 from our lab stock.

3.2. Taxol crystallization

On an ice bath GTP and Taxol were diluted in PEM80 buffer for a final concentration of 1 mM and 100 μM respectively, the solution was vortexed and incubated for 30 min at room temperature for a complete Taxol crystallization.

3.3. Taxol crystals labeled with rhodamine tubulin or rhodamine actin

The protein (rhodamine tubulin or actin) was added to the solution containing Taxol crystals for a final concentration of 0.1 mg/ml, then the solution was mixed and incubated for 30 minutes at 37 °C. Subsequently the samples were rinsed.

3.4. Taxol crystals labeled with fluorochromes: rhodamine, Cy3 and Alexa Fluor 488

The fluorochrome was added to the solution containing Taxol crystals for a final concentration of 5 μM, then the solution was mixed and incubated for 30 min at room temperature. Subsequently the samples were rinsed.

3.5. Rinsing of taxol spherulites in solution

100 μl of the solution to rinse were centrifugated at 120,000 rpm for 30 s. 50 μl of supernatant were then aspired and the pellet was resuspended in 50 μl of pure water.

This process was repeated for several times until the concentration of the fluorescent dye in the supernatant was undetected. Two extra cycles were preformed in order two surpass the detection limit of the equipment (2 ng/μl). Usually the rinsing process was accomplished in six cycles.

The effectiveness of the rinsing was verified measuring the concentration of the fluorescent molecules in the supernatant by means of light absorption using a spectrophotometer Nanodrop 1000 from Thermo Scientific.

3.6. Fluorescent microscopy

The fluorescent samples were observed in an Olympus inverted fluorescent microscope model IX71 using a excitation emission of 494 nm for the Alexa fluor 488 and 540 nm for Cy3 and Rhodamine. The images were taken with a 100× oil lens.

3.7. DIC microscopy

The samples were analyzed in a Nikon eclipse TE200 microscope using a 100x oil lens. Images were recorded in a VHS cassette and digitalized for the extraction of images.

3.8. FESEM

For scanning electron microscopy required a rinsing of the solutions to remove salts that are present in the buffer. Then a drop

of the solution was deposited on a cooper TEM grid coated with carbon and then dessicated at 37 °C during 40 min. The specimens containing proteins were previously fixed using a solution with 3% glutaraldehyde in PIPES buffer for one hour. All samples were metallized with Pt by sputtering coating with a thickness of approximately 7 nm. The images were taken using a Hitachi S-4800 field emission scanning electron microscope.

3.9. Computational methods

To find and evaluate new possible Taxol-binding sites in the tubulin dimer molecule we have followed a three-step approach. In the first step a fast rigid molecular docking of Taxol molecule to tubulin dimer using the FTDock v2.0 software with default parameters was performed [22]. Tubulin dimer (pdb code: 1jff) was digitized onto a $320\times320\times320$ grid with the resolution of 0.39 Å. Two conformations of Taxol were used, namely the conformation of Taxol in water solution [23], and T-Taxol conformation found in the native site of the tubulin dimer [21]. In the second step the sites with high scores from the docking experiments were evaluated on their hydrophobicity using the empirical atomic hydrophobicity scale [24] as implemented in the molsurfer software [25]. In this step the sites found in the first step were digitized onto a 99×99 map with the resolution of 0.25 Å.

The third step consisted of the flexible molecule docking using the AutoDock 4.0 software [26]. Both Taxol conformers were docked to the tubulin sites found in the first step of this computational approach. In each case prior to docking studies polar hydrogens were added and all histidine residues were made neutral and Kollman charges were assigned to all atoms [27]. The affinity grids were centered on each of the candidates for active sites with 0.203 Å spacing. We selected the Solis & Wets local search scheme for ligand conformational searching. For each case, the docking parameters were as follows: trials of 250 dockings, population size of 150, random starting position and conformation, a maximum of 300,000,000 iterations that the local search procedure applies to the phenotype of any given individual with 1000 successes or failures in a row before the algorithm adjusts variance, the initial variance of 1.0 with 0.01 lower bound and 0.06 probability of performing a local search on an individual.

To evaluate the rhodamine/fluorescein – Taxol interaction energies we have used a combined molecular mechanics – semiempirical approach. In the first step we have performed a series of fast minimizations of both systems in the amber f99 force field [28], starting from a set of 100 geometries with different fluorescent agent — Taxol orientations. In the second step the lowest-energy structure for each case has been subject to semiempirical PM6 calculations [29], as implemented in MOPAC2007 software (J.J.P. Stewart, MOPAC2007 Version 8.197 W, Stewart Computational Chemistry, 2007). Since the pKa value for the carboxylic groups of both rhodamine and fluorescein is close to the neutral pH value we have performed the calculations for both the deprotonated and protonated systems. The interaction energy between Taxol and fluorescent agent has been defined as the total energy of these separate systems subtracted from the total energy of the interacting system.

Acknowledgements

We acknowledge financial support from NSF/NIRT Grant 0303863.

We thank K. Visscher for access to his DIC microscope, S. Klewer for access to his laboratory, D. Loy, S. Patrick and A. Hoying for assisting in laboratory methods and D. Mastropaolo for sending us the coordinates of the crystallographic structures of Taxol.

References

[1] D.G.I. Kingston, Phytochemistry 68 (2007) 1844.
[2] M.C. Wani, H.L. Taylor, M.E. Wall, P. Coggon, A.T. McPhail, J. Am. Chem. Soc. 93 (1971) 2325.
[3] T.H. Wang, H.S. Wang, Y.K. Soong, Cancer 88 (2000) 2619.
[4] M.A. Jordan, L. Wilson, Nat. Rev. Cancer 4 (2004) 253.
[5] Y.W. Li, Y.J. Zhou, J. Zhu, C.H. Zheng, M. Zhang, C.Q. Sheng, J. Chinese U 27 (2006) 2084.
[6] H. Xiao, P. Verdier-Pinard, N. Fernandez-Fuentes, B. Burd, R. Angeletti, A. Fiser, S.B. Horwitz, G.A. Orr, Proc. Nal. Acad. Sci. U. S. A. 103 (2006) 10166.
[7] Q.Y. Sun, L. Lai, G.M. Wu, K.W. Park, B.N. Day, R.S. Prather, H. Schatten, Mol. Reprod. Dev. 60 (2001) 481.
[8] F. Verde, J.M. Berrez, C. Antony, E. Karsenti, J. Cell Biol. 112 (1991) 1177.
[9] G. Callaini, M.G. Riparbelli, Cell Motil. Cytoskelet. 37 (1997) 300.
[10] O.V. Zatsepina, A. Rousselet, P.K. Chan, M.O. Olson, E.G. Jordan, M. Bornens, J. Cell Sci. 112 (1999) 455.
[11] H. Nilsson, M. Wallin, Cell Motil. Cytoskelet. 41 (1998) 254.
[12] J. Szebeni, C.R. Alving, S. Savay, Y. Barenholz, A. Priev, D. Danino, Y. Talmon, Int. Immunopharmacol. 1 (2001) 721.
[13] R.T. Liggins, W.L. Hunter, H.M. Burt, J. Pharm. Sci. 86 (1997) 1458.
[14] R. Shi, H.M. Burt, Int. J. Pharm. 271 (2004) 167.
[15] M. Foss, B.W. Wilcox, C.-G. Alsop, D. Zhang, PLOS One 3 (2008) e1476.
[16] A.E. Mathew, M.R. Mejillano, J.P. Nath, R.H. Himes, J. Stella, J. Med. Chem. 35 (1992) 145.
[17] J.J. Manfredi, J. Parness, S.B. Horwitz, J. Cell Biol. 94 (1982) 688.
[18] J.R. Stehn, G. Schevzov, G.M. O'Neill, P.W. Gunning, Curr. Cancer Drug Targets 6 (2006) 245.
[19] D. Mastropaolo, A. Camermanm, Y. Luo, G.D. Brayer, N. Camerman, Proc. Natl. Acad. Sci. U. S. A. 92 (1995) 6920.
[20] J.P. Snyder, J.H. Nettles, B. Cornett, K.H. Downing, E. Nogales, Proc. Natl. Acad. Sci. U. S. A. 98 (2001) 5312.
[21] A. Lakdawala, M. Wang, N. Nevins, D.C. Liotta, D. Rusinska-Roszak, M. Lozynski, J.P. Snyder, BMC Chem. Biol. 1 (2001) 1.
[22] H.A. Gabb, R.M. Jackson, M.J. Sternberg, J. Mol. Biol. 272 (1997) 106.
[23] J. Dubois, D. Guenard, F. Guerittevoegelein, N. Guedira, P. Potier, B. Gillet, J.C. Beloeil, Tetrahedron 49 (1993) 6533.
[24] D. Eisenberg, M. Wesson, M. Yamashita, Chem. Scr. 29A (1989) 217.
[25] R.R. Gabdoulline, R.C. Wade, D. Walther, Nucleic Acids Res. 31 (2003) 3349.
[26] G.M. Morris, D.S. Goodsell, R.S. Halliday, R. Huey, W.E. Hart, R.K. Belew, A.J. Olson, J. Comput. Chem. 19 (1998) 1639.
[27] S.J. Weiner, P.A. Kollman, D.A. Case, U.C. Singh, C. Ghio, G. Alagona, S. Profeta, P. Weiner, J. Am. Chem. Soc. 106 (1984) 765.
[28] J. Wang, P. Cieplak, P.A. Kollman, J. Comput. Chem. 12 (2000) 1049.
[29] J.J.P. Stewart, J. Mol. Model 13 (2007) 1173.
[30] W. Humphrey, A. Dalke, K. Schulten, J. Mol. Graph. 14 (1996) 33.